Available online at www.sciencedirect.com
ScienceDirect
Physics of the Earth and Planetary Interiors 162 (2007) 149–163
PHYSICS OF THE EARTH AND PLANETARY INTERIORS
www.elsevier.com/locate/pepi

Some dynamical consequences of partial melting in Earth's deep mantle

John W. Hernlund *, Paul J. Tackley [1]

Department of Earth and Space Sciences, University of California, Los Angeles, CA 90095-1567, USA

Received 15 February 2007; received in revised form 2 April 2007; accepted 4 April 2007

Abstract

We use regional scale numerical models of mantle convection to investigate the simple hypothesis that seismically anomalous thin patches of Earth's lowermost mantle, termed "ultralow-velocity zones" or ULVZ, are derived from partial melting of ordinary mantle. The models span the lower 500 km of Earth's mantle, employ both temperature and melting-related contributions to buoyancy, and include a cold randomly moving downwelling introduced from above to maintain a thermal boundary layer. Partial melting of ordinary mantle introduces a ubiquitous partially molten layer above an isothermal core–mantle boundary as a consequence of its isothermal and isobaric conditions, although it naturally develops variations in thickness greater than two orders of magnitude, with the thickest portions occurring at the base of upwelling plumes and a thin layer elsewhere. We find that only a dense partially molten mixture produces partial melt distributions that are compatible with seismic observations of ULVZ; however, if such a melt percolates downward a dense basal liquid layer accumulates above the core–mantle boundary. The apparent requirement of a volumetrically dense and non-percolating melt phase in the lowermost mantle presents serious problems for the hypothesis that ULVZ arise from melting of ordinary mantle, and suggests that such features likely form as a consequence of more complex processes. Furthermore, these considerations suggest that the solidus of ordinary mantle is a reasonable upper bound on the present day temperature of the CMB.

Keywords: Ultralow-velocity zone; Core–mantle boundary; D″; Lower mantle; Partial melting; Mantle convection

1. Introduction

The proposition that 5–40 km thick portions of the lowermost mantle are partially molten (Williams and Garnero, 1996) may carry significant implications for the thermo-chemical state of the core–mantle boundary (CMB) region and provide important insights into the structure and dynamics of the lowermost mantle (Lay et al., 2004). Seismological studies indicate that seismic waves passing at or in close proximity to the CMB in some regions exhibit substantially reduced seismic wave velocities, which have been termed "ultralow-velocity zones" or "ULVZ" (Garnero and Helmberger, 1996). The inference of partial melt is based upon a reported three times stronger reduction in shear wave velocity relative to compressional wave velocity (Williams and Garnero, 1996), with estimated melt fractions falling between 5 and 30% depending upon whether the melt forms a well-connected or poorly connected topology (Berryman, 2000).

ULVZ are often implied to be limited in lateral extent (Lay et al., 2004), and some attempts have been made to systematically map their distribution at the CMB (e.g.,

* Corresponding author. Present address: Institut de Physique du Globe de Paris, 4 Place Jussieu, 75252 Paris Cedex 05, France.
E-mail address: hernlund@ipgp.jussieu.fr (J.W. Hernlund).
[1] Present address: Institute for Geophysics, ETH-Zurich, Hönggerberg HPP L13, Schafmattstrasse 30, 8093 Zurich, Switzerland.

0031-9201/$ – see front matter © 2007 Published by Elsevier B.V.
doi:10.1016/j.pepi.2007.04.005

Thorne and Garnero, 2004). However, other studies have argued for the existence of a very thin (ca. 1 km) ubiquitous global layer of partial melt away from ULVZ based on the analysis of high-frequency seismic waves (Revenaugh and Meyer, 1997; Garnero and Jeanloz, 2000; Ross et al., 2004). Studies with somewhat lower effective resolutions ($\approx$ 3 km), on the other hand, failed to find a similar ubiquitous signal along the CMB (Persh et al., 2001). Therefore, in order for ULVZ to simply be a thicker manifestation of an otherwise ubiquitous global thin partial melt layer, substantial variations in its thickness are required with the thinnest portions perhaps being significantly smaller than 3 km and the thickest portions being as much as several tens of km in vertical extent. ULVZ are usually inferred to be more dense than surrounding mantle (Rost and Revenaugh, 2003; Rost et al., 2005); however, a large uncertainty still exists in a variety of seismic studies (e.g., those employing diffracted phases) due to trade-offs in seismic properties (Williams and Garnero, 1996). Variations in thickness of a dense basal layer must be supported by correlated variations in patterns of deformation in the lowermost mantle, and such observations therefore carry important implications for the dynamics of the core–mantle boundary region.

The internal structure of ULVZ might also be heterogeneous. Strong lateral heterogeneity and anisotropy at the very base of the mantle in some regions might be associated with ULVZ-related processes (Garnero et al., 2004). Additionally, recent results indicate that the basal layer, where detected, does not always exhibit the characteristic three times reduction in S-wave velocity relative to P-waves (e.g., Avants et al., 2006), and therefore may not be partially molten in all locations. The tops of ULVZ do not always reflect seismic waves in a manner consistent with discontinuous jumps in seismic velocity, implying a diffuse upper boundary (Reasoner and Revenaugh, 2000; Persh et al., 2001; Rondenay and Fischer, 2003). However, notable examples of strong reflections have also been found, such as the southwest Pacific where a combination of constraints may yield density estimates for ULVZ (Rost et al., 2005).

ULVZ appear to be strongest in regions that are correlated with surface hot spot volcanism (Williams et al., 1998), suggestive of ULVZ being rooted beneath deep-seated mantle plumes arising from the D″ region (Morgan, 1971). Indeed, Helmberger et al. (1998) argued that the presence of a ULVZ $\approx$ 40 km thick and 250 km wide beneath the North Atlantic lends credibility to the hypothesis that a deep-seated mantle plume is responsible for the hotspot volcanism in Iceland. Locations of detected ULVZ are correlated with a combination of strong lateral seismic velocity gradients and low seismic velocity in D″ (Luo et al., 2001; Thorne et al., 2004) that predominantly occur along the edges of the two large low shear velocity provinces (LLSVPs) in the lower mantle beneath the Pacific (e.g., Romanowicz and Gung, 2002) and Africa (e.g., Wen, 2001). Torsvik et al. (2006) recently argued that the edges of LLSVPs are highly correlated with the original locations of LIPs for the past 200 million years. The origin of these LLSVPs has been attributed to a variety of mechanisms, such as large "superplumes" arising due to a strong increase in thermal conductivity with temperature (Matyska et al., 1994), plume "clusters" caused by the sweeping up of smaller thermal instabilities by the large-scale mantle circulation (Schubert et al., 2004), or the accumulation of chemically distinct material which is swept into piles by the mantle circulation (e.g., Tackley, 1998). The latter hypothesis has received a great deal of attention from the mantle dynamics community (e.g., Christensen, 1984; Davies and Gurnis, 1986; Hansen and Yuen, 1988; Sleep, 1988; Olson and Kincaid, 1991; Gurnis, 1986; Christensen, 1989; Kellogg and King, 1993; Tackley, 1998, 2002; Nakagawa and Tackley, 2004; Xie and Tackley, 2004a, b; McNamara and Zhong, 2004), and appears to be compatible with the observed seismic heterogeneity of the lowermost mantle (Tackley, 2002; McNamara and Zhong, 2005), the analysis of coupled variations in shear and bulk wave speeds that require compositional as well as thermal variations in these regions (e.g., Trampert et al., 2004), and may satisfy some geochemical constraints if these piles represent reserviors of subducted oceanic crust (e.g., Christensen and Hoffmann, 1994; Coltice and Ricard, 1999; Xie and Tackley, 2004a, b). Lay et al. (2006) recently argued that the detection of a lens of post-perovskite in the mid-Pacific LLSVP probably requires it to be chemically distinct (perhaps enriched in Fe) in order for this type of structure to occur in both seismically fast and slow regions of D″.

The preferential accumulation of ULVZs at the edges of LLSVPs is easily explained if they are chemically distinct piles of material. This is because any object embedded along the core–mantle boundary (e.g., ULVZ) will be carried with the mantle circulation and tend to accumulate where this flow field converges. Dense piles of material naturally develop an internal counter-circulation (e.g., Kellogg and King, 1993) such that mantle flow along the core–mantle boundary converges at the edges (Fig. 1), in accordance with observations (Luo et al., 2001). On the other hand, accumulation of ULVZ at the edges of LLSVPs is not straightforwardly explained if these features represent large "super-plumes" or plume clusters, which predict that ULVZ should be strongest directly beneath LLSVPs.

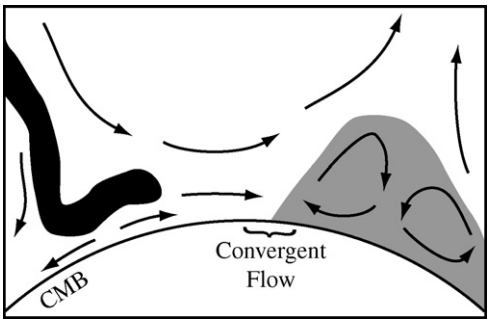

Fig. 1. Schematic illustration of the counter-circulation induced by the plate-scale mantle flow inside a dense chemical pile (grey) in the lowermost mantle (e.g., Kellogg and King, 1993). The mantle flow (arrows) is driven predominantly by the buoyancy of subducted oceanic lithosphere (black). A matching of velocities at the pile edge requires downwelling flow in the middle of the pile and a return flow along the core–mantle boundary (CMB) such that the pile edges are a location of preferential flow convergence. Any object embedded along the CMB (e.g., ULVZ) will therefore be preferentially deposited at pile edges.

Several mechanisms for producing partial melts at the CMB have been proposed. The simplest is partial melting of the mantle itself (Williams and Garnero, 1996). The uncertainties for the temperature of the CMB as well as the deep mantle solidus are likely large enough to to permit this scenario, though some (e.g., Boehler, 2000) have argued that the core may be too cool, and the solidus too high to allow for this possibility. In its simplest form, this would lead to ubiquitous melting of the lowermost mantle where the geotherm intersects the solidus just above the CMB (Revenaugh and Meyer, 1997), or be concentrated by localized processes, e.g., magma chamber-like heat pumps (Morse, 2001). Others (e.g., Helffrich and Kaneshima, 2004) have argued that the solidus must be an upper bound on core temperature, because the distribution of partial melting that would occur cannot be consistent with the observed seismic heterogeneity in D″. Duffy and Ahrens (1992), on the other hand, argue for the extensive presence of small degrees of partial melt throughout the lowermost mantle to explain decoupled P- and S-wave velocity variations. Partial melting of abnormally fertile "chunks" of mantle is another possibility. It has been suggested that portions of subducted ocean crust may melt at CMB conditions, even if a "typical" pyrolite (or its residuum) does not produce significant amounts of melt (Ohtani and Maeda, 2001; Jellinek and Manga, 2004).

It is to be expected that any chemical segregation accompanying partial melting in the deep mantle would create an observable geochemical signal that might be detected at the surface, e.g., in hotspot volcano products associated with deep-seated mantle plumes. An enrichment of the melt phase in iron and radiogenic elements such as uranium relative to $MgSiO_3$-perovskite has been reported in diamond anvil cell experiments (Knittle, 1998). Recent experiments on trace element partitioning between expected lower mantle phase assemblages and melt have shown that many otherwise incompatible elements (e.g., the large ion lithophile elements) will preferentially partition into $CaSiO_3$-perovskite (Corgne and Wood, 2002; Hirose et al., 2004). Some of the expected geochemical signals have been shown to be consistent with those observed in some volcanic products (Hirose et al., 2004); however, it is not straightforward to distinguish whether this is due to ongoing or past melting events in the lower mantle.

Core–mantle reactions are another possibility for creating a thin layer of dense material which might explain the occurrence of ULVZ (Manga and Jeanloz, 1996). Several different reactions between solid mantle components and the outer core have been proposed (e.g., Knittle and Jeanloz, 1991; Dubrovinsky et al., 2001, 2004), whose products should generally be a mixture of solids and liquids (Walker et al., 2002). Considerable debate has arisen regarding whether Pt/Re/Os systematics observed in some hot spot volcano products represent firm evidence of core–mantle reactions (e.g., Brandon and Walker, 2005, and references therein).

Solid "sediments" might crystallize within, and rise upward from, a light element saturated outer core and compact onto the base of the mantle (Buffett et al., 2000). This kind of mechanism is designed to produce a given electrical conductivity profile in the CMB region to explain core–mantle electro-magnetic coupling, and is not meant to specifically account for the origin of ULVZ. However, it is another way of producing a mixture of partly liquid material, which might then be swept into concentrated piles by the larger-scale mantle circulation impinging upon the core–mantle boundary.

Other mechanisms have also been proposed to account for the presence of ULVZ. Steinbach and Yuen (1999) suggested that viscous heating in the conduit of rising plumes could lead to temperatures greater than the core–mantle boundary, possibly leading to partial melting of the mantle in a manner that does not require the presence of melt away from plumes. Melting of subducted Archean banded-iron formations formed as a consequence of atmospheric oxidation and exsolution of iron in the oceans has also been posited (Dobson and Brodholt, 2005); however, it is unclear whether this kind of material in the form of a thin veneer atop subducting slabs would be able to segregate from the bulk mantle flow, and whether the volume would be sufficient to retain a persistent layer in the presence of continual mantle entrainment by convection currents (e.g., Sleep,

1988) over a time scale that is roughly half the age of Earth. Recently, Mao et al. (2006) proposed that Fe-rich post-perovskite forming at the base of the mantle could account for the anomalous properties of ULVZ without requiring the presence of partial melt. However, it is not clear whether post-perovskite is stable at the very base of the mantle (Hernlund et al., 2005) even in regions that are modestly enriched in Fe (Lay et al., 2006). On the other hand, more extreme Fe-enrichment in a thin veneer above the CMB might stabilize post-perovskite, but raises questions regarding whether it would in fact be a solid at CMB temperatures.

The above-mentioned mechanisms are not mutually exclusive, nor are they necessarily exhaustive. Indeed, it would be surprising if only one were responsible for producing materials with distinct chemical and physical properties at the CMB. For example, chemical components originating from the core could be mixed into the lower mantle and cause "fluxed" partial melting. The mantle clearly exhibits a finite range of chemical heterogeneity, and it is not reasonable to suppose that all of the present varieties would be in chemical equilibrium with the outer core if they were brought into contact at the CMB by convection. Thus some degree of chemical reactions are inevitable; however, the nature of any reaction products remains less certain.

One important difference between a chemically distinct and mantle phase change origin for ULVZ is the expected density anomaly that would result. ULVZ produced by a phase change (e.g., partial melting) of ordinary mantle cannot differ from the surrounding mantle density by more than a few percent without straining credibility, while chemically distinct ULVZ could have much greater density depending upon the bulk chemistry. If we assume that ULVZ is a mixture of typical lower mantle silicate solids (specific density of 5.5) and an unknown fluid ranging from a mantle partial melt (within a few % of mantle density) to pure outer core fluid (specific density of 9.9), then it is straightforward to show how the fluid composition influences the overall ULVZ bulk density. This is shown schematically in Fig. 2, where a range of 5–30% in fluid fraction is imposed as an additional constraint (Berryman, 2000). A maximum ULVZ specific density of around 6.8 is implied by this example, while a minimum of around a couple percent smaller than ordinary mantle density is a reasonable lower bound.

Because most observations of ULVZ are made using seismic phases that diffract along the core–mantle boundary, some uncertainties can arise in interpreting whether observed ULVZ lie mostly in the mantle, or perhaps represent structure entirely at the top of the outer core (e.g., Thorne and Garnero, 2004). To a very good

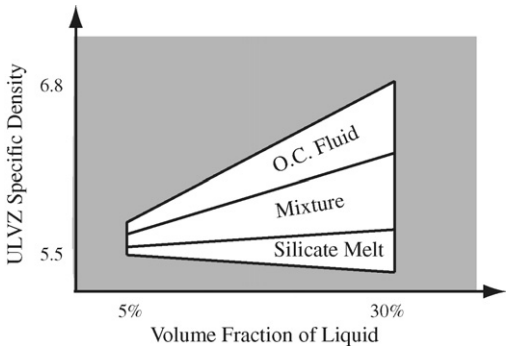

Fig. 2. Plausible range of ULVZ densities in terms of the nature of the component liquid ("O.C." is outer core), assuming the solid components are ordinary silicates with densities similar to the ambient lower mantle and applying a possible liquid fraction in the range 5–30% (Berryman, 2000). The grey area comprises parameter combinations that are not possible under the given assumptions.

approximation, ULVZ should maintain isostatic equilibrium as a consequence of the low viscosity expected of material at the high temperatures of the CMB (see Fig. 3). Consider a ULVZ of total thickness h and density ρ_u intermediate between the core ρ_c and mantle ρ_m, i.e. $\rho_m < \rho_u < \rho_c$. The thickness of the portion of ULVZ inside the mantle h_m and inside the core h_c $(= h - h_m)$ are then related to one another by a simple column density balance, i.e. $h_c(\rho_c - \rho_u) = h_m(\rho_u - \rho_m)$. If ULVZ density is more than a few percent higher than ordinary mantle, significant protrusions of ULVZ into the outer core are to be expected where they become thicker. For the upper bound of $\rho_u \approx 6.8$ estimated above, the effective core side topography of such protrusions is as high as 2/5 the mantle side topography. This could be large enough to overwhelm the contribution of dynamic topography along the core–mantle boundary, which is expected to vary by up to 2 km in the vicinity of upwelling plumes (e.g., Olson et al., 1987). However,

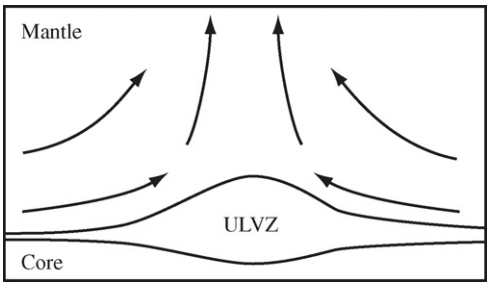

Fig. 3. Illustration of the isostatic balance expected to be maintained by ULVZ embedded along the CMB. An increased mantle-side thickness will be accompanied by a compensatory core–side protrusion. Prevention of the flattening out of ULVZ must be maintained by mantle flow, shown schematically by the arrows.

ULVZ will cause a depression of the core–mantle interface beneath upwellings while dynamic topography has the opposite tendency, and so the net effect could actually be a lessening (or reversal) of the expected amplitude of core–mantle boundary topography. A particular ULVZ location probed recently by Rost et al. (2005) has an inferred thickness of 8.5 km and density anomaly of 10%, which should contribute 1 km of variation to CMB topography due to isostasy alone.

Much attention regarding the physical implications of ULVZ has been focused upon the core. In particular, angular momentum exchange between the core and mantle detected as decadal variations in the length of day can be explained by an electro-magnetic torque exerted upon the base of the mantle in an electrically conductive layer (e.g., Buffett, 1996). Although ULVZ appear to be an attractive option for producing this effect, Poirier et al. (1998) have shown that the necessary conductivity increase could only arise from metal infiltration into the mantle from the core, a process which they estimate cannot attain the necessary thickness required to achieve a sufficient total conductance. Other mechanisms to enhance the thickness of penetration of core material into the mantle have recently been proposed, such as the suction mechanism of Kanda and Stevenson (2006), or shear-induced transfer mechanisms that rely upon poro-elasticity (Petford et al., 2005). The core sediment mechanism of Buffett et al. (2000) is designed to circumvent the apparent difficulty of iron entrainment by offering a continuous flux of solids from below; however, this mechanism requires small grain sizes. A layer formed by such a mechanism would inevitably be deformed and transported by mantle flow to become preferentially deposited where it converges along the CMB. The resultant lateral variability in conductance could have effects on core dynamics that might explain (Runcorn, 1992; Aurnou et al., 1996) the proposed existence of preferred geomagnetic reversal paths (Clement, 1991; Laj et al., 1991; Costin and Buffett, 2004). While this mechanism alone may be too weak to explain all the data (Brito et al., 1999), it is not the sole candidate because heat flux and/or CMB topography variations could have similar influences upon preferred reversal paths (e.g., Gubbins, 1998), if such patterns actually exist and are not simply artifacts of uneven data sampling (e.g., Valet et al., 1992).

To date, relatively little attention has been paid to the dynamical implications of ULVZ for mantle processes. Manga and Jeanloz (1996) considered the dynamical consequences of a high thermal conductivity layer arising from an increased abundance of metals in a variable thickness chemical boundary layer, and argued that it would help to stabilize the base of upwelling thermal plumes and increase lateral temperature variations in the lowermost mantle. However, the possibility of a large increase in thermal conductivity in ULVZ has been challenged by Poirier et al. (1998), for reasons similar to those facing high electrical conductivity. Farnetani (1997) showed that a thin dense layer results in a reduced excess temperature in the axis of upwelling plumes, perhaps explaining why plume temperatures inferred from a variety of observations beneath hot spot swells are much lower than the expected temperature change across the D″ thermal boundary layer. Jellinek and Manga (2002) used laboratory convection experiments including a dense chemical layer to suggest that dense material helps to fix the location of upwelling plumes, which is a requirement for such plumes to exhibit "hot-spot-like" behavior at Earth's surface. Jellinek and Manga (2004) have shown that entrainment of a dense basal layer should imply a relationship between the chemistry and buoyancy flux of plumes, and argue that a layer composed of both mantle and core derived material is consistent with observations. Recently, Okamoto et al. (2005) considered the effects of partial melting upon seismic anisotropy arising from shape-preferred orientation in transient convection models; however, in their study partial melting was a purely passive process and was allowed to take place throughout D″.

In this study, the dynamical effects associated with partial melting of ordinary mantle are considered in order to better understand the consequences of such a process occurring in the lowermost mantle, and to evaluate to what extent such a process might contribute to ULVZ-related seismic structure. Regional-scale numerical models of mantle convection are used which allow the details of the lowermost mantle to be adequately resolved. It will be shown that only a dense partially molten region appears to be compatible with observations. However, due to the long timescales involved, we find that allowing any degree of melt percolation in ULVZ under these conditions leads to excessive accumulation of silicate melt at the CMB. Thus we argue that ULVZ are likely not formed by simple melting of ordinary mantle at the present time.

2. Numerical model

The setting for the models considered here is the lowermost 500 km of the mantle, in which a cold downwelling "slab" introduced from above produces and interacts with a thermal boundary layer above an impenetrable isothermal outer core. The flow is driven entirely by buoyancy forces arising from temperature and partial

melt fraction variations. This allows the characteristics of the flow to arise in a self-consistent manner with a minimum number of imposed restrictions. The top of the domain is permeable to flow, which allows the imposed "slab" to freely enter the domain while at the same time permitting upwelling material to escape from the top. In contrast to other kinds of models, such as the consideration of the inherently transient growth and subsequent instability of a thermal boundary layer, this approach allows quasi-steady solutions to be obtained that better represent the characteristics of well-developed convection.

2.1. Governing equations

The code STAG3D (Tackley, 1996) is used to solve the equations expressing conservation of mass, momentum, energy, and melt fraction:

$$\vec{\nabla} \cdot \vec{v} = 0, \tag{1}$$

$$2\vec{\nabla} \cdot (\mu \vec{\nabla} \vec{v}) + \vec{\nabla} \times (\mu \vec{\nabla} \times \vec{v}) - \vec{\nabla} p = \hat{z}(RaT + Rm\phi), \tag{2}$$

$$\frac{\partial T}{\partial t} + \vec{v} \cdot \vec{\nabla} T = \nabla^2 T - L\dot{M}, \tag{3}$$

$$\frac{\partial \phi}{\partial t} + \vec{v} \cdot \vec{\nabla} \phi = -\frac{\partial}{\partial z}[(1-\phi)u] + \dot{M}, \tag{4}$$

where $\vec{\nabla}$ is the gradient vector, $\vec{v}$ the bulk velocity (average of effective melt $\vec{v}_\mathrm{m}$ and solid $\vec{v}_\mathrm{s}$ velocities), μ the viscosity, p the dynamic pressure, T the temperature, ϕ the volume fraction of melt, t the time, L the latent heat of melting, and $\dot{M}$ is the rate of melting. The equations have been non-dimensionalized relative to a density ρ_0, length scale D, time scale D^2/κ (κ is the thermal diffusivity), temperature scale ΔT, and viscosity μ_0, and both the Boussinesq and infinite Prandtl number approximations are assumed. Ra and Rm are defined as

$$Ra = \frac{\rho_0 g \alpha \Delta T D^3}{\kappa \mu_0}, \tag{5}$$

$$Rm = -\frac{g D^3}{\kappa \mu_0}\left(\frac{\partial \rho}{\partial \phi}\right), \tag{6}$$

where g is the gravitational acceleration and α is the thermal expansivity. It will also be useful to define a non-dimensional buoyancy number:

$$B = -\frac{Rm\phi_\mathrm{max}}{Ra}, \tag{7}$$

which describes the (negative) buoyancy of partially molten material at the maximum melt fraction ϕ_max relative to thermal buoyancy. For simplicity, the Darcy velocity, u, is modeled as,

$$u\hat{z} = \phi(\vec{v}_\mathrm{m} - \vec{v}_\mathrm{s}) = \frac{Rm}{Mr}\phi^2 \hat{z}, \tag{8}$$

where the parameter Mr is defined by,

$$Mr = \frac{\mu_\mathrm{m} D^2}{\mu_0 k_0}, \tag{9}$$

where μ_m is the melt viscosity, and k_0 is a reference Darcy permeability. Mr is inversely proportional to the rate of percolation, and is termed a "melt retention number." This simple description of percolation assumes that the Darcy permeability is given by $k = k_0\phi^2$, which is only valid for small melt fractions. However, this assumption will not affect the basic results, which will be seen to be independent of the form of the Darcy velocity so long as it increases with melt fraction.

The viscosity is taken to be Newtonian and temperature dependent, and follows a thermally activated Arrhenius relationship of the form:

$$\mu = \exp\left(\frac{E_\mathrm{a}}{T + T_0} - \frac{E_\mathrm{a}}{T_0 + T_\mathrm{ref}}\right), \tag{10}$$

where E_a is a non-dimensional activation energy (normalized by the gas constant R and ΔT), T_0 the non-dimensionalized absolute temperature at the model temperature $T = 0$, and T_ref is the non-dimensional reference temperature for which $\mu = 1$, which is chosen to be $T_0 = 1/2$. For the activation energy, a dimensional value of 336 kJ/mol is used, appropriate for diffusion creep of silicate perovskite (Yamazaki and Karato, 2001). For the adopted dimensional parameter values $T_0 = \Delta T = 2000$ K used in this study, Eq. (10) yields a total viscosity variation of 2.4×10^4.

The governing equations are solved in a two-dimensional domain of aspect-ratio 4. The grid density utilized in the model is 64 cells in the vertical direction and 256 cells in the horizontal direction. Grid refinement is also implemented so that the vertical resolution is increased by a factor of 2 at the base of the model domain. For a domain height of 500 km, this gives a vertical resolution of about 4 km at the core–mantle boundary.

2.2. Melting model

A simple melting model is employed with a solidus temperature T_s that does not vary with pressure. The pressure dependence of the real mantle solidus is not well-constrained at the relevant pressures, though it is probably small over length scales of 5–40 km. The extent of melting is tracked using a "fertility" c, which measures

the fraction of melt that can be extracted from the solid. The fertility is a property of the solid, and obeys the conservation equation:

$$\frac{\partial c}{\partial t} + \vec{v} \cdot \vec{\nabla} c = \frac{\partial (uc)}{\partial z} - \dot{M}. \quad (11)$$

When melt is present, the temperature and fertility are confined to a linear melting trajectory:

$$T_m - T_s = \frac{c_0 - c}{c_0}(T_c - T_s), \quad (12)$$

where c_0 is the initial value of c and T_m is the temperature in the presence of melt. The value c_0 is also equivalent to the maximum fraction of melt that can be produced at the CMB temperature T_c. Melting or freezing takes places whenever the temperature T departs from T_m, yielding an excess energy $\Delta e = T - T_m$. The conservation of energy then requires that:

$$\Delta e = \Delta T_m - L\Delta c = \left(\frac{\partial T_m}{\partial c} - L \right) \delta c, \quad (13)$$

and from Eq. (12),

$$\delta\phi = -\delta c = \frac{c_0 \delta e}{c_0 L + T_c - T_s}. \quad (14)$$

2.3. Boundary conditions

The side boundaries of the model domain are enforced to be periodic, and the bottom is isothermal and free-slip. The top is insulating and permeable; however, a Gaussian temperature anomaly having a half-width of 50 km is imposed at the top of the domain. Instead of specifying the temperature directly, the coldest portion of the anomaly is taken to be $T = 0$ and the temperature of the CMB is $T = 1$, so that the relevant ΔT in our non-dimensionalization is the difference in temperature between the CMB and the slab. In order to mimic the random nature of downwellings in the lowermost mantle and introduce extra time dependence in the system, the location of the imposed "slab" is made to perform a random walk with a small move δx in the positive or negative x-direction of equal likelihood at each time step. Permeability of the upper boundary is implemented in a manner similar to previous studies using the code STAG3D, such as the introduction of an upwelling thermal plume from the bottom of the model domain (Moore et al., 1998). Permeability is enforced by setting the non-isostatic part part of the model pressure to zero along the upper boundary, and requiring that the vertical gradient in each velocity component vanishes. The upper boundary condition for the fertility is set to c_0, which causes material entering the domain (i.e., downwellings) to be capable of producing the maximum degree of melt. This boundary condition has no effect on upwelling material leaving the top of the domain.

3. Results

Table 1 lists the parameter values used in this study. The reference viscosity, thermal diffusivity, thermal expansivity, and other quantities involved in the thermal Rayleigh number were taken to be fixed for most of the cases presented here. While we have explored variations in the Rayleigh number, the basic findings of the models do not change in significant ways. We have also found that modest variations in viscosity with respect to melt fraction do not change the basic structure of the solutions, particularly when the layer is thin enough to be comparable to ULVZ, thus in the present paper only temperature variations affect viscosity. In combination with the randomly moving slab, the reference value of $Ra = 1.375 \times 10^5$ is large enough to induce time-dependent convection. The effective volume averaged Rayleigh number was typically about 3×10^4 in the model runs. The melt buoyancy parameter B was varied from -1 to 3, which when combined with the other parameters yields a ULVZ density variation ranging from -110 to 330 kg/m^3 (or -2% to 6% relative to unmelted mantle). The use of this range of values for B was guided by exploratory modeling over a larger range of buoyancy numbers.

Fig. 4 shows the variation in the types of partially molten structures produced for a range of B and T_s when no melt percolation occurs (i.e. $Mr = \infty$). In these cases, ϕ is simply correlated with $T - T_s$; however,

Table 1
Parameter values considered in this study (ND stands for non-dimensional)

Quantity	Value	Units
ρ_0	5500	kg/m^3
g	10	m/s^2
E_a	336	kJ/mol
μ_0	10^{21}	Pa s
α	10^{-5}	K^{-1}
ΔT	2000	K
κ	10^{-6}	m^2/s
D	500	km
Mr	10^0– 10^8, ∞	ND
Ra	1.375×10^5	ND
B	-1 to 3	ND
T_{ref}	0.5	ND
T_0	1.0	ND
T_s	0.8–0.95	ND
ϕ_{max}	0.3	ND

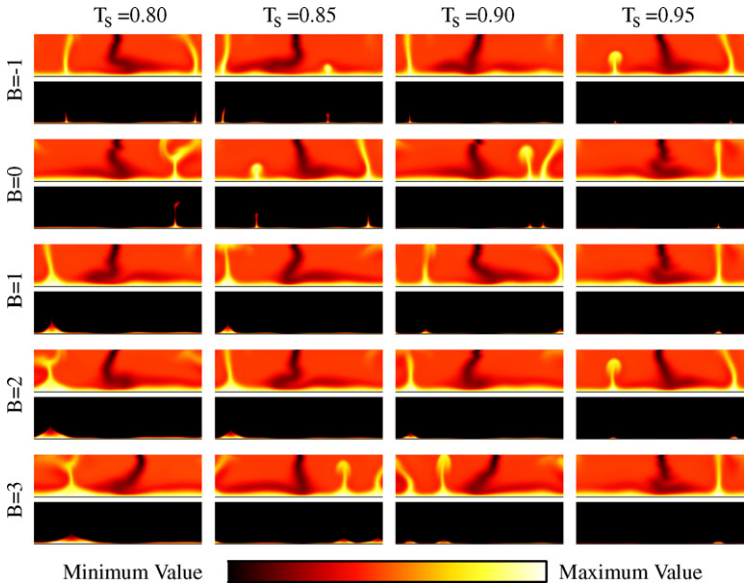

Fig. 4. Plots of temperature (top plot in each pair) and melt fraction (bottom plot in each pair) showing the typical structures that occur for various values of T_s and B when there is no percolation and the maximum melt fraction is 30%.

the buoyancy of the partially molten mixture and the solidus temperature influence the overall shape of partially molten regions at the base of upwelling plumes. Thicker partially molten structures are favored by a smaller value of T_s and/or B. The buoyancy number controls the aspect ratio of the thick partial melt zone that accumulates at the base of upwelling thermal plumes, with larger values of B inducing a wider base, and neutral or buoyant melt (i.e. for $B = 0, -1$) producing very narrow concentrations of melt primarily as tendrils within plume axes. Neutral or less dense melt produces structures having an aspect ratio less than unity, while a dense melt can be significantly wider than it is tall. The thickness of the partially molten zone is very thin away from upwelling thermal plumes regardless of melt buoyancy, and is thinnest beneath the downwelling "slab." Fig. 5 shows how the time average of the maximum thickness of the partially molten layer depends upon T_s and B. Only higher values of T_s and B yield thicknesses which fall in a plausible ULVZ-like range of 50 km or less.

The melt retention number Mr was varied by more than eight orders of magnitude to assess the consequences of melt percolation. For cases with $B < 0$ (buoyant melting), the partial melt was found to separate from the base of the model domain, and either rises upward and freezes or entirely leaves the top of the domain. Fig. 6 shows the effects of finite melt percolation for a case where the melt is dense. A dense melt drains downward and accumulates at the bottom to form a 100% melt layer. Fig. 7 shows the range of parame-

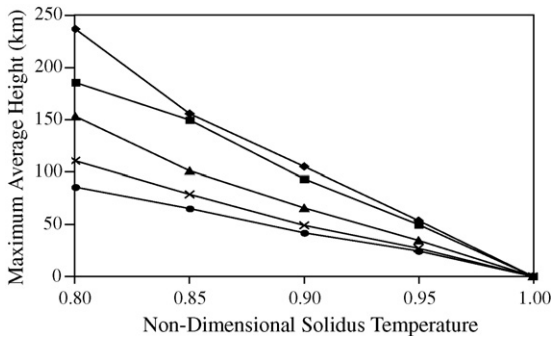

Fig. 5. Plot of the average maximum height of partial melt above the bottom of the domain (in km) as a function of the non-dimensional solidus temperature for buoyancy number values of $B = -1$ (diamonds), $B = 0$ (squares), $B = 1$ (triangles), $B = 2$ (crosses), and $B = 3$ (circles) when there is no melt percolation. The theoretical value of zero melt height for a solidus temperature of unity is also plotted.

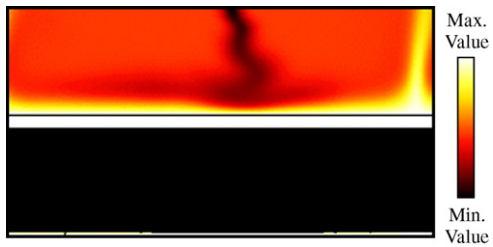

Fig. 6. A typical result for a case with a significant degree of percolation, for which the melt rapidly drains into a 100% melted layer at the base of the domain.

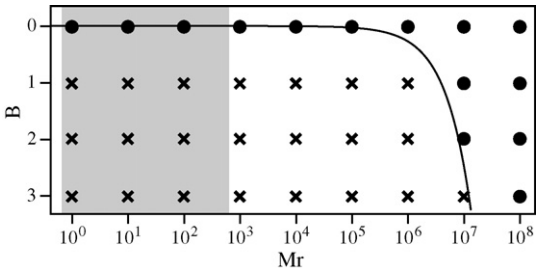

Fig. 7. The distribution of cases where a 100% melt layer develops (crosses) as a function of B and Mr for a value of $T_s = 0.8$ with cases that do not develop such a layer also shown (circles). Similar behavior is found for any value of T_s. The high values of Mr required to suppress this drainage suggest that any significant degree of dense melt percolation will give rise to a 100% melt layer. The curved line shows the predicted behavior of this system if a time scale for percolative drainage of melt is what fundamentally controls this process, and the region shaded in grey shows the expected range of values for Mr using typical ranges of physical parameters (see Section 4).

ters over which a 100% melt layer accumulates. Only for zero melt buoyancy or for extremely large values of Mr can the development of a significant (i.e. $>$ 10 km thick) 100% melt layer be avoided. For $Mr > 10^7$, effective melt velocities are on the order of 10^{-4} to 10^{-3}, in which case there is essentially no melt percolation occurring on the time scale of the model runs. If these runs are allowed to continue, the thickness of the melt layer continues to grow since new "fertile" material is introduced from above and the melting temperature does not decrease with height. At some later time the layer reaches an equilibrium thickness; however, this result is not robust since the low viscosity expected of such a melt layer is not included in the present models.

Few significant systematic differences in heat flow and plume temperature have been found to arise in these kinds of models when partial melt is included (Hernlund, 2006). This is especially true for cases that yield variations in melt thickness that are most compatible with seismic observations of ULVZ. Furthermore, since we shall argue in the next section that this particular model already presents serious problems for the notion that ULVZ can be formed by melting of ordinary mantle, we do not find it appropriate to explore a detailed analysis of its characteristics.

4. Discussion

The results presented above show that ULVZ could be explained as a thicker manifestation of a ubiquitous dense partial melt layer resulting from a core temperature that exceeds the mantle solidus. However, as we will argue below, the partially molten region must be more dense than its co-existing solids and additionally cannot be allowed to percolate through the pore spaces it occupies in the matrix. Both of these issues present problems for the hypothesis that partial melting of ordinary mantle can occur at the present time in Earth's core–mantle boundary region.

4.1. Density and shape of partially molten regions

The above modeling results show that the density of the partially molten region exerts a strong influence upon its morphology. In particular, partial melts that are neutral or less dense tend to form tall, narrow tendrils in the axes of upwelling plumes. This effect might be amplified even further if viscous heating were significant (Steinbach and Yuen, 1999). The only reason this melt is not entirely swept up into the plumes, as a compositionally distinct less dense "blob" of material would do, is that it is able to freeze when the plume axis cools sufficiently at some finite distance above the core–mantle boundary. Dense melting, on the other hand, gives rise to structures with a wide base and smaller thickness.

It would be difficult to argue with any certainty that the axes of upwelling plumes do not contain tall, thin conduits of partial melt in the deeper mantle due to the fundamental resolution limitations of tele-seismic waves. However, the areal distribution of the thickness of lower density partial melt layers at the core–mantle boundary presents a problem because they are very thin everywhere except directly beneath upwelling plumes. As a consequence, these kinds of structures might also be difficult to detect at the core–mantle boundary for exactly the same reason that they would be difficult to detect in plume axes at shallower depths. This is because diffracted waves travelling along the core–mantle interface would not spend a significant amount of time in regions where partial melt is thick enough to result in anomalously late travel time arrivals. This type of distribution would also be difficult to reconcile with the observed regional depressions in seismic wave velocity that are often identified as "ULVZ." For these reasons, a partially melted region that is more dense than unmelted material appears to be more compatible with observations than scenarios where they are less dense, and in any case will be required to contribute significantly to the observed seismic heterogeneity at the base of the mantle.

The requirement that partially molten mantle must obtain a greater density than unmelted mantle to contribute to observed seismic heterogeneity might at first glance seem to be problematic from a material physics point of view. However, dense melting has been observed

and rigorously studied in a variety of materials at high pressure (Liu and Bassett, 1986), and has also been posited to occur in the lowermost upper mantle of Earth (Rigden et al., 1984; Agee and Walker, 1988, 1993; Ohtani et al., 1993; Suzuki et al., 1995; Agee, 1998; Ohtani and Maeda, 2001; Suzuki and Ohtani, 2003; Sakamaki et al., 2006). There are two ways to induce dense partially molten regions: (1) by melting to a liquid with an intrinsically smaller molar volume, or (2) by preferentially partitioning elements with the greatest mass into the liquid phase and then concentrating the melt by percolation and subsequent segregation. The latter possibility runs into difficulties, however, if the degree of melt percolation (discussed further below) must be negligibly small to avoid excessive melt accumulation at the core–mantle boundary. This is because in the absence of percolation the melt does not segregate from the solid, and therefore robbing the latter of heavier elements leads to a complementary reduction in solid mass and hence no bulk (melt + solid) density change arises solely as a consequence of differential element partitioning. Therefore the first possibility, that the melt has an intrinsically smaller molar volume than the original solid material that produced it, is the only viable option if dense melting is required and there is no significant degree of melt percolation.

In the simplest case of congruent melting, where a solid melts to a liquid of identical composition, solid–liquid density crossovers usually occur at pressures just below a solid–solid–liquid triple phase junction, a phenomenon which is often attributed to the melt having partial atomic configurations similar to the higher pressure solid phase at pressures smaller than the solid–solid phase change would occur (Liu and Bassett, 1986). This causes a characteristic depression in melting temperature near the triple point, which is shown schematically in Fig. 8 and is well understood thermodynamically in terms of the Clapeyron relation:

$$\frac{\mathrm{d}T_\mathrm{m}}{\mathrm{d}P} = \frac{\Delta V_\mathrm{m}}{\Delta S_\mathrm{m}}, \tag{15}$$

where in this context T_m is the congruent melting temperature, P the pressure, and ΔV_m and ΔS_m are the respective volume and entropy changes upon melting. Thus a change in ΔV_m from positive to negative values associated with a density crossover is associated with a local maxima in the melting curve. ΔS_m must always be positive, since melt is the higher temperature phase.

On the basis of shock wave experiments, Akins et al. (2004) argued for dense congruent melting of $MgSiO_3$-perovskite at pressures of the D″ layer, with a density crossover occurring at slightly lower pressures

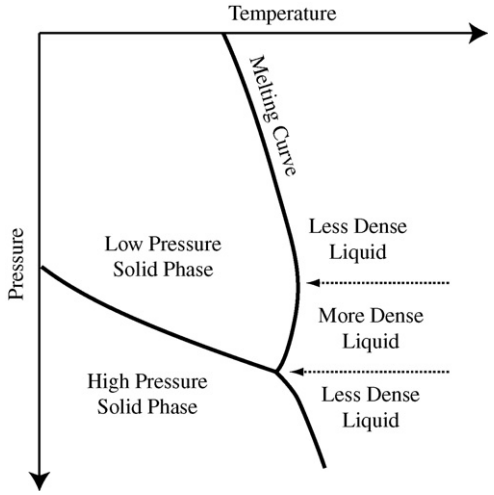

Fig. 8. Schematic illustration of a melting curve depression arising as the consequence of a density crossover due to the proximity of a solid–solid–liquid triple point. The dotted arrows indicate where melt changes from being less dense than the solid to more dense, or vice versa.

(ca. 80 GPa). Given the probable volumetric importance of silicate perovskite in lower mantle mineral assemblages, this effect might account for a modest volume decrease (higher density) in a partially molten ULVZ. The recent discovery of a post-perovskite phase of $MgSiO_3$ (Murakami et al., 2004; Oganov and Ono, 2004; Tsuchiya et al., 2004) provides for an additional higher pressure solid phase that would facilitate the occurrence of a triple phase junction analogous to the scenario illustrated in Fig. 8. However, the solid phase change itself might complicate the interpretation of the shock wave data used by Akins et al. (2004). Recent ab initio calculations support the notion of a rapidly increasing Si–O coordination (from 4 to 6) in $MgSiO_3$ liquid with pressure under lower mantle conditions (Stixrude and Karki, 2005); however, they do not support the occurrence of $\Delta V_\mathrm{m} < 0$ at any pressures, which would be required to induce a dense partially molten region in the absence of percolation. Instead, Stixrude and Karki (2005) support the notion that the melt can only be more dense than the solid if it preferentially consumes heavier oxides (e.g., FeO), and as a consequence dense partially molten regions of the deep mantle can only arise after significant amounts of melt segregation has occurred.

4.2. Absence of percolation?

Fig. 9 illustrates the basic reason why the presence of any degree of melt percolation through the solid matrix leads to the growth of a 100% melt layer in the models. In order to avoid drainage by percolation, melt must

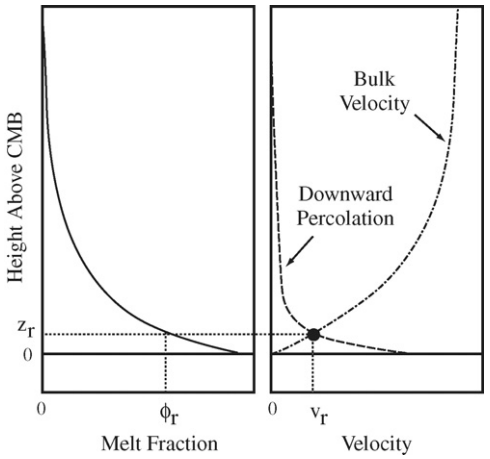

Fig. 9. Schematic illustration of the reason why any degree of melt percolation inevitably accumulates a 100% partially molten layer at the core–mantle boundary. The left plot shows how the partial melt profile (solid line) induced by temperature alone must typically increase with depth, while the right plot shows profiles of the bulk mantle upwelling velocity (dot-dashed line) and downward rate of melt percolation (dashed line). Because the upward bulk velocity must be zero at the CMB, there will always exist some region of height z_r where a fraction of melt greater than ϕ_r leads to a downward rate of percolation faster than the upwelling flow, v_r. The melt in the layer beneath z_r will drain to the CMB and form a silicate melt layer.

be transported upward by the bulk mantle circulation at a rate equal to (or greater than) the downward melt velocity. However, the bulk upward velocity is necessarily zero at the core–mantle boundary. Partial melt, on the other hand, is correlated with temperature, which increases downward toward the core–mantle boundary, so that a finite degree of partial melt is maintained at the very bottom of the mantle. Thus there is inevitably some region below which the upward velocity is too small to overcome a finite rate of downward melt percolation. Because the dense melt travels toward the core–mantle boundary in a convergent flow, it accumulates into a melt layer which thickens over time. In detail, a compaction boundary layer of order 1 km might form above this mantle-derived melt; however, this effect is not resolved in the present models. According to conservation Eq. (4) with a Darcy velocity given by Eq. (8), the characteristic time scale for draining a layer melt is proportional to Mr/B. Requiring that the time scale be larger than some critical value then leads to a simple proportionality $B \propto Mr$ separating scenarios where melt is rapidly drained from those where partial melt is retained. This is plotted against the results in Fig. 7, showing that the timescale for percolative draining is what fundamentally controls whether or not any partial melt is retained in the solids within the boundary layer. Also shown is a plausible guess for the plausible range of Mr using extreme values of melt viscosity (upper bound of 10 Pa s) and Darcy permeability (lower bound of 10^{-11} m^2). Because these are poorly constrained parameters, the current estimates may be highly inaccurate; however, the error would need to compensate 4 orders of magnitude increase in Mr.

Any restriction against significant rates of melt percolation presents an enigma for the possibility that ULVZ are a stable mixture of liquid and solid, regardless of whether or not it derives from partial melting of the mantle itself. On the one hand, this might be explained as the result of a lack of inter-connectedness of the melt phase in the matrix (i.e., the grain boundaries are not "wetted" by the melt). However, this would carry implications for seismically inferred ULVZ melt fractions, favoring higher estimates (i.e., 30%) in a poorly connected melt topology (Berryman, 2000), which in turn also requires the effective "wetting fraction" of melt to be even higher. Another possibility is a high melt viscosity, although this is difficult to justify at the high temperatures of the CMB region. Physical and chemical interactions between ULVZ liquid and outer core liquid within the matrix might also play a role in preventing drainage of melt from the layer, or reactions in the liquid to form solid interstitial crystals that effectively "plug" the melt conduits (e.g., Rost et al., 2005). However, until there is ample theoretical and experimental justification for these kinds of mechanisms, any attempt to explain a lack of melt percolation must be considered inherently ad hoc.

The other option is that there does exist some degree of melt percolation, and a thin silicate melt layer forms over time near the CMB via drainage from the overlying mantle. The two fluids at the CMB could also react or mix to form a layer with a density intermediate between the remaining outer core fluid and a mantle-derived melt. The resultant fluid mixture would necessarily have a lower density than deeper outer core fluid, and might be immiscible with it depending upon the abundance of other alloying elements. Based on analysis of multiple $P4KP$ and PcP waveforms, Helffrich and Kaneshima (2004) argue that there is no large scale stratification in the outer core; however, they and Eaton and Kendall (2005) find that that a thin layer at the very top of the outer core (on the order to tens of km) might be consistent with observations, in agreement with earlier studies (e.g., Lay and Young, 1990). However, a layer of silicate melt has never been suggested to be the cause of such a layer.

Outermost core layers have previously been posited, such as a "stratified ocean of the core" (Braginsky, 1999), and has received attention because of its potential rela-

tion to styles of chemical and thermal convection in the outer core. All of these studies considered this layer to be composed either of liquid having only a slightly different composition from the average core (enriched in light elements), or arising as a consequence of a hot layer that would form when a greater amount of heat is transported along the core adiabat than is taken up into the overlying mantle (e.g., Labrosse et al., 1997; Lister and Buffett, 1998). However, recent estimates of CMB heat flow using post-perovskite phase relations in D″ (Hernlund et al., 2005; Lay et al., 2006; van der Hilst et al., 2007) are significantly greater than the conductive heat flow in the core, and thus a thermal stratification may be less likely. The presence of significant amounts of silicate melt would be expected to give rise to variations in seismic properties at the top of the core that may be too large to be supported by observations, so that substantial mixing of this material into the core would be required.

Alternatively, dense melt could drain downward and accumulate at some small distance above the CMB if there exists a thin layer of material with a density greater than the melt at the CMB. However, a melt-rich layer would still form due to its convergent flow, causing it to increase in thickness over time if it is fed by ongoing melting processes in the overlying mantle. Without large degrees of entrainment and re-freezing of this material back into the overlying mantle this scenario still presents problems for the hypothesis that ULVZ are produced by partial melting of ordinary mantle. Instead, a limited supply of fertile material, and hence melt, might be required in order that such a layer remains reasonably thin.

Another important consequence of percolation is that it can give rise to chemical segregation and an accompanying geochemical signature. Without percolation, there will be no geochemical signal induced by melting in the deep mantle, because material ascending upward (where it could be probed) would simply freeze and presumably re-equilibrate to form an assemblage identical to that which it possessed prior to melting. Segregation, or the lack thereof, might also carry dynamical implications because changes in chemistry in the residual solid material following melt extraction could give rise to solid density variations that would in turn influence the buoyant flow regime in the deep mantle.

5. Summary and conclusion

The models performed in this study demonstrate that ULVZ might be a thicker manifestation of an otherwise very thin and dense partial melt layer at the CMB which arises due to a solidus that is lower than the outermost core temperature by about 100–200 K. However, an apparent paradox arises because on the one hand, partially molten layers produce ULVZ-like structures only when they are dense, yet the expected downward percolation of a dense melt leads to drainage and melt accumulation that might be difficult to reconcile with observations of Earth at the present time.

It must be emphasized that this study only considered the consequences of partial melting of ordinary mantle material, and many other complex scenarios can be envisioned. A further promising direction would be to consider the slow crystallization of a primordial dense residual portion of the magma ocean over time as suggested by Stixrude and Karki (2005), in which case the problem is one of freezing and fractionating a layer of melt instead of producing melt from the mantle itself. Clearly, other alternatives also exist, such as the possibility that ULVZ are not actually a mixture of liquid and solid.

Acknowledgements

Preliminary reviews by Abby Kavner, Paul Roberts, and Gerald Schubert greatly improved the manuscript. We are also grateful for discussions with Mark Jellinek, William B. Moore, and Stéphane Labrosse. This work was supported in part by a grant from IGPP Los Alamos.

References

Agee, C.B., 1998. Crystal-liquid density inversions in terrestrial and lunar magmas. Phys. Earth Planet. Int. 107, 63–74.

Agee, C.B., Walker, D., 1988. Static compression and olivine flotation in ultrabasic silicate liquid. J. Geophys. Res. B 93, 3437–3449.

Agee, C.B., Walker, D., 1993. Olivine flotation in mantle melt. Earth Planet. Sci. Lett. 114, 315–324.

Akins, J.A., Luo, S-N., Asimow, P.D., Ahrens, T.J., 2004. Shock-induced melting of $MgSiO_3$ and implications for melts in Earth's lowermost mantle. Geophys. Res. Lett. 31, L14612.

Aurnou, J.M., Buttles, J.L., Neumann, G.A., Olson, P.L., 1996. Electromagnetic core–mantle coupling and paleomagnetic reversal paths. Geophys. Res. Lett. 23, 2705–2708.

Avants, M., Lay, T., Garnero, E.J., 2006. Determining shear velocity structure of the ULVZ beneath the central Pacific using stacked *ScS* data. Geophys. Res. Lett. 33, L07314.

Berryman, J.G., 2000. Seismic velocity decrement ratios for regions of partial melt in the lower mantle. Geophys. Res. Lett. 27, 421–424.

Boehler, R., 2000. High-pressure experiments and the phase diagram of lower mantle and core constituents. Rev. Geophys. 38, 221–245.

Braginsky, S.I., 1999. Dynamics of the stably stratified ocean at the top of the core. Phys. Earth Planet. Int. 111, 21–34.

Brandon, A.D., Walker, R.J., 2005. The debate over core–mantle interaction. Earth Planet. Sci. Lett. 232, 211–225.

Brito, D., Aurnou, J., Olson, P., 1999. Can heterogeneous core–mantle electromagnetic coupling control geomagnetic reversals? Phys. Earth Planet. Int. 112, 159–170.

Buffett, B.A., 1996. A mechanism for decade fluctuations in the length of day. Geophys. Res. Lett. 23, 3803–3806.

Buffett, B.A., Garnero, E.J., Jeanloz, R., 2000. Sediments at the top of the Earth's core. Science 290, 1338–1342.

Christensen, U., 1984. Instability of a hot boundary-layer and initiation of thermo-chemical plumes. Ann. Geophys. 2, 311–319.

Christensen, U.R., 1989. Models of mantle convection—one or several layers. Phil. Trans. R. Soc. Lond. A 328, 417–424.

Christensen, U.R., Hoffmann, A.W., 1994. Segregation of subducted oceanic crust in the convecting mantle. J. Geophys. Res. B 99, 19867–19884.

Clement, B.M., 1991. Geographical distribution of transitional VGPs: evidence for non-zonal equatorial symmetry during the Matuyama–Brunhes geomagnetic reversal. Earth Planet. Sci. Lett. 104, 48–58.

Coltice, N., Ricard, Y., 1999. Geochemical observations and one layer mantle convection. Earth Planet. Sci. Lett. 174, 125–137.

Corgne, A., Wood, B.J., 2002. $CaSiO_3$ and $CaTiO_3$ perovskite-melt partitioning of trace elements: Implications for gross mantle differentiation. Geophys. Res. Lett. 29, 1933.

Costin, S.O., Buffett, B.A., 2004. Preferred reversal paths caused by a heterogeneous conducting layer at the base of the mantle. J. Geophys. Res. 109, B06101.

Davies, G.F., Gurnis, M., 1986. Interaction of mantle dregs with convection—lateral heterogeneity at the core mantle boundary. Geophys. Res. Lett. 13, 1517–1520.

Dobson, D.P., Brodholt, J.P., 2005. Subducted banded iron formations as a source of ultralow-velocity zones at the core–mantle boundary. Nature 434, 371–374.

Dubrovinsky, L., Annerstin, H., Dubrovinskaia, N., 2001. Chemical interaction of Fe and Al_2O_3 as a source of heterogeneity at the Earth's core–mantle boundary. Nature 412, 527–529.

Dubrovinsky, L., Dubrovinskaia, N., Langenhorst, F., 2004. Reaction of iron and silica at core–mantle boundary conditions. Phys. Earth Planet. Int. 146, 243–247.

Duffy, T., Ahrens, T.J., 1992. Lateral variation in lower mantle seismic velocity. In: Syono, Y., Manghnani, M.H. (Eds.), High Pressure Research: Application to Earth and Planetary Sciences. Terra Scientific, pp. 197–205.

Eaton, D.W., Kendall, J.-M., 2005. Improving seismic resolution of outermost core structure by multichannel analysis and deconvolution of broadband SmKS phases. Phys. Earth Planet. Int. 155, 104–119.

Farnetani, C.G., 1997. Excess temperature of mantle plumes: the role of chemical stratification across D″. Geophys. Res. Lett. 24, 1583–1586.

Garnero, E.J., Helmberger, D.V., 1996. Seismic detection of a thin laterally varying boundary layer at the base of the mantle beneath the central-Pacific. Geophys. Res. Lett. 23, 977–980.

Garnero, E.J., Jeanloz, R., 2000. Fuzzy patches on the Earth's core–mantle boundary? Geophys. Res. Lett. 27, 2777–2780.

Garnero, E.J., Maupin, V., Lay, T., Fouch, M.J., 2004. Variable azimuthal anisotropy in Earth's lowermost mantle. Science 306, 259–261.

Gubbins, D., 1998. Interpreting the paleomagnetic field. In: Gurnis, M., Wysession, M.E., Knittle, E., Buffett, B.A. (Eds.), The Core–Mantle Boundary Region. American Geophysical Union Monograph, pp. 167–182.

Gurnis, M., 1986. The effects of chemical density differences on convective mixing in the Earth's mantle. J. Geophys. Res. B 91, 1407–1419.

Hansen, U., Yuen, D.A., 1988. Numerical simulations of thermal-chemical instabilities at the core mantle boundary. Nature 334, 237–240.

Helffrich, G., Kaneshima, S., 2004. Seismological constraints on core composition from Fe–O–S liquid immiscibility. Science 306, 2239–2242.

Helmberger, D.V., Wen, L., Ding, X., 1998. Seismic evidence that the source of the iceland hotspot lies at the core–mantle boundary. Nature 396, 251–255.

Hernlund, J.W., 2006. Dynamics Associated with Partial Melting in Earth's Uppermost and Lowermost Mantle and the Structure and Phase Relationships in Earth's D″ Layer. University of California, Los Angeles.

Hernlund, J.W., Thomas, C., Tackley, P.J., 2005. A doubling of the post-perovskite phase boundary and structure of the Earth's lowermost mantle. Nature 434, 882–886.

Hirose, K., Shimuzu, N., van Westrenen, W., Fei, Y., 2004. Trace element partitioning in Earth's lower mantle and implications for geochemical consequences of partial melting at the core–mantle boundary. Phys. Earth Planet. Int. 146, 249–260.

Jellinek, A.M., Manga, M., 2002. The influence of a chemical boundary layer on the fixity, spacing, and lifetime of mantle plumes. Nature 418, 760–763.

Jellinek, A.M., Manga, M., 2004. Links between long-lived hot spots, mantle plumes, D″, and plate tectonics. Rev. Geophys. 42, 3002.

Kanda, R.V.S., Stevenson, D.J., 2006. Suction mechanism for iron entrainment into the lower mantle. Geophys. Res. Lett. 33, L02310.

Kellogg, L.H., King, S.D., 1993. Effect of mantle plumes on the growth of D″ by reaction between the core and mantle. Geophys. Res. Lett. 20, 379–382.

Knittle, E., 1998. The solid/liquid partitioning of major and radiogenic elements at lower mantle pressures: implications for the core–mantle boundary region. In: Gurnis, M., Wysession, M.E., Knittle, E., Buffett, B.A. (Eds.), The core–Mantle Boundary Region. American Geophysical Union Monograph, pp. 119–130.

Knittle, E., Jeanloz, R., 1991. The Earth's core–mantle boundary: results of experiments at high pressures and temperatures. Science 251, 1438–1443.

Labrosse, S., Poirier, J.-P., Le Mouël, J.-L., 1997. On cooling of the earth's core. Phys. Earth Planet. Int. 99, 1–17.

Laj, C., Mazaud, A., Weeks, R., Fuller, M., Herrero-Bervera, E., 1991. Geomagnetic reversal paths. Nature 351, 447.

Lay, T., Young, C.J., 1990. The stably-stratified outermost core revisited. Geophys. Res. Lett. 17, 2001–2004.

Lay, T., Garnero, E.J., Williams, Q., 2004. Partial melting in a thermo-chemical boundary layer at the base of the mantle. Phys. Earth Planet. Int. 146, 441–467.

Lay, T., Hernlund, J., Garnero, E.J., Thorne, M.S., 2006. A post-perovskite lens and D″ heat flux beneath the central Pacific. Science 314, 1272–1276.

Lister, J.R., Buffett, B.A., 1998. Stratification of the outer core at the core–mantle boundary. Phys. Earth Planet. Int. 105, 5–19.

Liu, L., Bassett, W.A., 1986. Elements, Oxides, Silicates: High-Pressure Phases with Implications for the Earths Interior. Oxford University Press.

Luo, S.-N., Ni, S., Helmberger, D.V., 2001. Evidence for a sharp lateral variation of velocity at the core–mantle boundary from multipathed PKPab. Earth Planet. Sci. Lett. 189, 155–164.

Manga, M., Jeanloz, R., 1996. Implications of a metal-bearing chemical boundary layer in D″ for mantle dynamics. Geophys. Res. Lett. 23, 3091–3094.

Mao, W.L., Mao, H-K., Sturhahn, W., Zhao, J., Prakapenka, V.B., Shu, J., Fei, Y., Hemley, R.J., 2006. Iron-rich post-perovskite and the origin of ultralow-velocity zones. Science 312, 564–565.

Matyska, C., Moser, J., Yuen, D.A., 1994. The potential influence of radiative heat transfer on the formation of megaplumes in the lower mantle. Earth Planet. Sci. Lett. 125, 255–266.

McNamara, A.K., Zhong, S., 2004. Thermochemical structures within a spherical mantle: superplumes or piles? J. Geophys. Res. B 109, B07402.

McNamara, A.K., Zhong, S., 2005. Thermochemical piles under Africa and the Pacific. Nature 437, 1136–1139.

Moore, W.B., Schubert, G., Tackley, P., 1998. Three-dimensional simulation of plume–lithosphere interaction at the Hawaiian swell. Science 279, 1008–1011.

Morgan, W.J., 1971. Convection plumes in the lower mantle. Nature 230, 42–43.

Morse, S.A., 2001. A double magmatic heat pump at the core–mantle boundary. Am. Mineral. 85, 387–390.

Murakami, M., Hirose, K., Sata, N., Ohishi, Y., Kawamura, K., 2004. Phase transition of $MgSiO_3$ perovskite in the deep lower mantle. Science 304, 855–858.

Nakagawa, T., Tackley, P.J., 2004. Thermo-chemical structure in the mantle arising from a three-component convective system and implications for geochemistry. Phys. Earth Planet. Int. 146, 125–138.

Oganov, A.R., Ono, S., 2004. Theoretical and experimental evidence for a post-perovskite phase of $MgSiO_3$ in Earth's D″ layer. Nature 430, 445–448.

Ohtani, E., Maeda, M., 2001. Density of basaltic melt at high pressure and stability of the melt at the base of the lower mantle. Earth Planet. Sci. Lett. 193, 69–75.

Ohtani, E., Suzuki, A., Kato, T., 1993. Flotation of olivine in the peridotite melt at high pressure. Proc. Jpn. Acad. Ser. B 69, 23–28.

Okamoto, T., Sumita, I., Nakakuki, T., Yoshida, S., 2005. Deformation of a partially molten D″ layer by small-scale convection and the resulting seismic anisotropy and ultralow velocity zone. Phys. Earth Planet. Int. 153, 32–48.

Olson, P., Kincaid, C., 1991. Experiments on the interaction of thermal-convection and compositional layering at the base of the mantle. J. Geophys. Res. B 96, 4347–4354.

Olson, P., Schubert, G., Anderson, C., 1987. Plume formation in the D″-layer and the roughness of the core–mantle boundary. Nature 327, 409–413.

Persh, S.E., Vidale, J.E., Earle, P.S., 2001. Absence of short-period ULVZ precursors to PcP and ScP from two regions of the CMB. Geophys. Res. Lett. 28, 859–862.

Petford, N., Yuen, D., Rushmer, T., Brodholt, J., Stackhouse, S., 2005. Shear-induced material transfer across the core–mantle boundary aided by the post-perovskite phase transition. Earth Planets Space 57, 459–464.

Poirier, J.P., Malavergne, V., Le Mouël, J.L., 1998. Is there a thin electrically conducting layer at the base of the mantle? In: Gurnis, M., Wysession, M.E., Knittle, E., Buffett, B.A. (Eds.), The core–Mantle Boundary Region. American Geophysical Union Monograph, pp. 131–137.

Reasoner, C., Revenaugh, J., 2000. ScP constraints on ultralow-velocity zone density and gradient thickness beneath the Pacific. J. Geophys. Res. B 105, 173–182.

Revenaugh, J., Meyer, R., 1997. Seismic evidence of partial melt within a possibly ubiquitous low-velocity layer at the base of the mantle. Science 277, 670–673.

Rigden, S.M., Ahrens, T.J., Stolper, E.M., 1984. Densities of liquid silicates at high pressures. Science 226, 1071–1073.

Romanowicz, B., Gung, Y., 2002. Superplumes from the core–mantle boundary to the lithosphere: implications for heat flux. Science 296, 513–516.

Rondenay, S., Fischer, K.M., 2003. Constraints on localized core–mantle boundary structure from multichannel, broadband SKS coda analysis. J. Geophys. Res. B 108, 2537.

Ross, A.R., Thybo, H., Solidilov, L.N., 2004. Reflection seismic profiles of the core–mantle boundary. J. Geophys. Res. B 109, B08303.

Rost, S., Revenaugh, J., 2003. Small scale ultralow velocity zone structure imaged by ScP. J. Geophys. Res. B 108, 2056.

Rost, S., Garnero, E.J., Williams, Q., Manga, M., 2005. Seismic constraints on a possible plume root at the core–mantle boundary. Nature 435, 666–669.

Runcorn, S.K., 1992. Polar path in geomagnetic reversals. Nature 356, 654–656.

Sakamaki, T., Suzuki, A., Ohtani, E., 2006. Stability of hydrous melt at the base of the earth's upper mantle. Nature 439, 192–194.

Schubert, G., Masters, G., Tackley, P.J., Olson, P., 2004. Superplumes or plume clusters? Phys. Earth Planet. Int. 146, 147–162.

Sleep, N.H., 1988. Gradual entrainment of a chemical layer at the base of the mantle by overlying convection. Geophys. J. 95, 437–447.

Steinbach, V., Yuen, D.A., 1999. Viscous heating: a potential mechanism for the formation of the ultralow velocity zone. Earth Planet. Sci. Lett. 172, 213–220.

Stixrude, L., Karki, B., 2005. Structure and freezing of $MgSiO_3$ liquid in Earths lower mantle. Science 310, 297–299.

Suzuki, A., Ohtani, E., 2003. Density of peridotite melts at high pressure. Phys. Chem. Miner. 30, 449–456.

Suzuki, A., Ohtani, E., Kato, T., 1995. Flotation of diamond in mantle melt at high pressure. Science 269, 216–218.

Tackley, P.J., 1996. Effects of strongly variable viscosity on three-dimensional compressible convection in planetary mantles. J. Geophys. Res. B 101, 3311–3332.

Tackley, P.J., 1998. Three-dimensional simulations of mantle convection with a thermo-chemical basal boundary layer: D″? In: Gurnis, M., Wysession, M.E., Knittle, E., Buffett, B.A. (Eds.), The Core–Mantle Boundary Region. American Geophysical Union Monograph, pp. 231–253.

Tackley, P.J., 2002. Strong heterogeneity caused by deep mantle layering. Geochem. Geophys. Geosyst. 3.

Thorne, M., Garnero, E.J., Grand, S., 2004. Geographic correlation between hot spots and deep mantle lateral shear-wave velocity gradients. Phys. Earth Planet. Int. 146, 47–63.

Thorne, M.S., Garnero, E.J., 2004. Inferences on ultralow-velocity zone structure from a global analysis of SPdKS waves. J. Geophys. Res. B 109, B08301.

Torsvik, T.H., Smethurst, M.A., Burke, K., Steinberger, B., 2006. Large igneous provinces generated from the margins of the large low-velocity provinces in the deep mantle. Geophys. J. Int. 167, 1447–1460.

Trampert, J., Deschamps, F., Resovsky, J., Yuen, D.A., 2004. Probabilistic tomography maps chemical heterogenities throughout the mantle. Science 306, 853–856.

Tsuchiya, T., Tsuchiya, J., Umemoto, K., Wentzcovitch, R.M., 2004. Phase transition in $MgSiO_3$ perovskite in the Earth's lower mantle. Earth Planet. Sci. Lett. 224, 241–248.

Valet, J.-P., Tucholka, P., Courtillot, V., Meynadier, L., 1992. Paleomagnetic constraints on the geometry of the geomagnetic field during reversal. Nature 356, 400.

van der Hilst, R.D., de Hoop, M.V., Wang, P., Shim, S.-H., Ma, P., Tenorio, L., 2007. Seismostratigraphy and thermal structure of Earth's core–mantle boundary region. Science 30, 1813–1817.

Walker, D., Clark, S.M., Cranswick, L.M.D., 2002. O_2 volumes at high pressure from $KClO_4$ decomposition: D″ as a siderophile element pump instead of a lid on the core. Geochem. Geophys. Geosyst. 3, 1070.

Wen, L., 2001. Seismic evidence for a rapidly-varying compositional anomaly at the base of the Earth's mantle beneath the Indian ocean. Earth Planet. Sci. Lett. 194, 83–95.

Williams, Q., Garnero, E.J., 1996. Seismic evidence for partial melt at the base of the Earth's mantle. Science 273, 1528–1530.

Williams, Q., Revenaugh, J.S., Garnero, E.J., 1998. A correlation between ultra-low basal velocities in the mantle and hot spots. Science 281, 546–549.

Xie, S., Tackley, P.J., 2004a. Evolution of helium and argon isotopes in a convecting mantle. Phys. Earth Planet. Int. 146, 417–439.

Xie, S., Tackley, P.J., 2004b. Evolution of U–Pb and Sm–Nd systems in numerical models of mantle convection. J. Geophys. Res. B 109, B11204.

Yamazaki, D., Karato, S.-I., 2001. Some mineral physics constraints on the rheology and geothermal structure of Earth's lower mantle. Am. Mineral. 86, 385–391.